GEOPHYSICAL RESEARCH LETTERS, VOL. 19, NO. 18, PAGES 1815-1818, SEPTEMBER 23, 1992

OPTICAL SIGNATURES OF LIGHTNING-INDUCED HEATING OF THE *D* REGION

Y.N. Taranenko, U.S. Inan, and T.F. Bell

Space, Telecommunications and Radioscience Laboratory, Stanford University, Stanford, California 94305

Abstract. Lightning-induced heating of the nighttime *D* region leads to the excitation of a number of lines of O, O_2, N_2, O_2^+, and N_2^+, at intensities of 10-10^9 Rayleighs (R) for vertical observations. For example, the 5577 Å emission from O has intensity ~60 R lasting for ~350 ms while the 1st and 2nd positive bands of N_2 are at ~10^9 R but last only ~50μs.

1. Introduction

Excitation of optical emissions should be a natural consequence of lightning-induced heating of ambient *D* region electrons to energies of several eV [*Inan et al.*, 1991]. Space Shuttle observations [*Boeck et al.*, 1992] of a transient airglow enhancement associated with a lightning discharge may be evidence of such optical emissions.

We employ here the *Inan et al.* [1991] model for lightning-induced heating to estimate radiation times and intensities of selected lines of O, O_2 and N_2 in a model atmosphere for different observing geometries, including that of *Boeck et al.* [1992].

2. Theoretical Formulation

We assume that ionospheric electrons are heated to 2 to 6 eV at ~93 km altitude with an exponential scale heights for temperature of 1.5 and 7 km respectively above and below, for ~50 μs. We neglect electron transport due to the short duration.

Our results are not sensitively dependent on the ambient electron density model and we adopt a 'typical' ambient nighttime *D* region electron density [*Reagan et al.*, 1981] shown in Figure 1.

The impact excitation of neutral species is given by:

$$\frac{\partial n_i}{\partial t} = -\frac{n_i}{\tau_i} + \sum_j n_j A_j + N_{0i} R_i \qquad (1)$$

where n_i is the density of excited particles at i-th level, N_{0i} is the ambient density of corresponding neutrals, $\tau_i = (\sum_l A_l + k_{1i}[N_2] + k_{2i}[O_2] + k_{3i}[O])^{-1}$ is the total lifetime of the i-th state (brackets denote concentration), A_l is the radiation transition rate, k_{ij} is the quenching rate, and R_i is the excited state source term.

The MSIS neutral atmosphere model [*Rees*, 1989, Appendix 1] (Figure 1) is adopted for densities of O, O_2 and N_2 as well as O_2^+ and N_2^+ ions produced via electron impact ionization of neutrals. Energy level diagrams of O, O_2, N_2, O_2^+, and N_2^+ are well known (e.g., see *Jones* [1974], pp. 85-91).

Paper number 92GL02106
0094-8534/92/92GL-02106$03.00

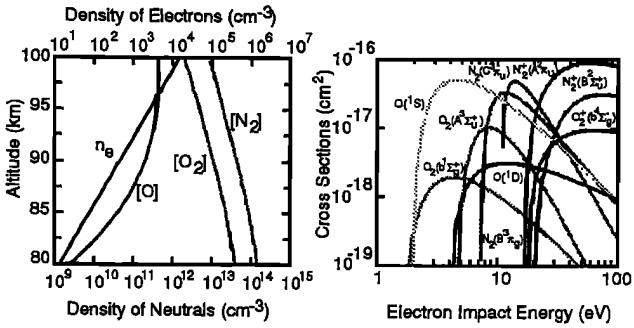

Fig. 1. (Left) Ambient midlatitude ionospheric profiles for the densities of electrons (n_e), atomic oxygen ([O]), molecular oxygen ([O_2]), and molecular nitrogen ([N_2]). Fig. 2. (Right) Excitation and ionization cross-sections for electron impact for states analyzed in this paper.

Each of these species has emission lines ranging from far infrared (IR) to extreme ultraviolet (UV) commonly observed in the aurora and airglow. Emission lines to be studied were selected using equation (1) and considering several factors such as; *(i)* electron impact cross-sections of the lines, *(ii)* emission rate of the excited levels, *(iii)* branching ratio of different lines originating from the same level, *(iv)* cascade and radiation trapping effects, (v) quenching rate by neutral species, and *(vi)* transparency of the atmosphere at the wavelength of the emission. Lines such as 1304 and 1356 Å of O were not considered since the medium is optically thick both upward and downward from ~ 93 km altitude.

We thus restrict our attention to the red 6300 (6364) Å ($^1D \rightarrow {}^3P$ transitions), and the green 5577 Å ($^1S \rightarrow {}^1D$) lines of O; the atmospheric band ($b^1\Sigma_g^+ \rightarrow X^3\Sigma_g^-$) and UV Herzberg I band ($A^3\Sigma_u^+ \rightarrow X^3\Sigma_g^-$) of O_2; the blue to UV 2nd positive band ($C^3\pi_u \rightarrow B^3\pi_g$) and red to IR 1st positive band ($B^3\pi_g \rightarrow A^3\Sigma_u^+$) of N_2; the blue 1st negative band ($B^2\Sigma_u^+ \rightarrow X^2\Sigma_g^+$) and IR Meinel band ($A^2\pi_u \rightarrow X^2\Sigma_g^+$) of N_2^+; and the red 1st negative band ($b^4\Sigma_g^- \rightarrow a^4\pi_u$) of O_2^+, all of which are regularly observed in the airglow aurora [*Jones*, 1974; *Chamberlain*, 1978].

The excitation cross-sections for these emissions as a function of electron energy are shown in Figure 2 whereas quenching and emission rates are summarized in Table 1. The data in Figure 2 were taken from: for ^1D and ^1S states of O [*Doering and Gulcicek*, 1989], for $b^1\Sigma_g^+$ and $A^3\Sigma_u^+$ states of O_2 [*Rees*, 1989, Appendix 4 and references therein], for $C^3\pi_u$ and $B^3\pi_g$ states of N_2 [*Cartwright et al.* 1977], for $A^2\pi_u$ and $B^2\Sigma_u^+$ states of N_2^+ [*Cartwright et al.* 1975], for $b^4\Sigma_g^-$ state of O_2^+ [*Watson et al.* 1967].

Comparison of radiation and quenching rates indicates that the 6300 and 5577 Å lines from O, and the atmospheric and Herzberg I bands from O_2, are quenched at *D*-region altitudes, while the other lines are not strongly quenched. Two

TABLE 1. Quenching and Emission Rates

Reaction	Rates ($cm^3\ s^{-1}$ or s^{-1})
$O(^1D) \rightarrow O + h\nu$	9.34×10^{-3}*
$O(^1D) + N_2 \rightarrow O + N_2$	$2.0 \times 10^{-11} \exp(107.8/T)$*
$O(^1D) + O_2 \rightarrow O + O_2$	$2.9 \times 10^{-11} \exp(67.5/T)$*
$O(^1D) + O \rightarrow O + O$	8×10^{-12}*
$O(^1S) \rightarrow O(^1D) + h\nu$	1.07*
$O(^1S) \rightarrow O + h\nu$	0.0444*
$O(^1S) + O_2 \rightarrow O + O_2$	$4.9 \times 10^{-12} \exp(-885/T)$*
$O(^1S) + O \rightarrow O + O$	2×10^{-14}*
$O_2(b^1\Sigma) \rightarrow O_2 + h\nu$	0.083†
(Atmospheric bands)	0.079†
$O_2(b^1\Sigma) + O \rightarrow O_2 + O$	8×10^{-14}†
$O_2(b^1\Sigma) + N_2 \rightarrow O_2 + N_2$	2.2×10^{-15}†
$O_2(A^3\Sigma) \rightarrow O_2 + h\nu$	6.25†
(Herzberg I bands)	3-7 (v' dependent)†
$O_2(A^3\Sigma) + O \rightarrow O_2 + O$	3×10^{-13}†
$O_2(A^3\Sigma) + N_2 \rightarrow O_2 + N_2$	3×10^{-13}†
$N_2(C^3\pi_u) \rightarrow N_2(B^3\pi_g) + h\nu$	2×10^7‡
$N_2(C^3\pi_u) + O_2 \rightarrow O_2 + N_2$	3×10^{-10}‡
$N_2(B^3\pi_g) \rightarrow N_2(A^3\Sigma_u^+) + h\nu$	1.7×10^5‡
$N_2(B^3\pi_g) + N_2 \rightarrow N_2 + N_2$	10^{-11}‡
$N_2^+(B^2\Sigma_u^+) \rightarrow N_2^+(X^2\Sigma_g^+) + h\nu$	1.4×10^6‡
$N_2^+(B^2\Sigma_u^+) + N_2 \rightarrow N_2 + N_2$	4×10^{-10}‡
$N_2^+(A^2\pi_u) \rightarrow N_2^+(X^2\Sigma_g^+) + h\nu$	7×10^4‡
$N_2^+(B^2\Sigma_u^+) + N_2 \rightarrow N_2 + N_2$	5×10^{-10}‡
$O_2^+(b^4\Sigma_g^-) \rightarrow O_2^+(a^4\pi_u) + h\nu$	8.5×10^4‡
$O_2^+(b^4\Sigma_g^-) + N_2 \rightarrow O_2 + N_2$	2×10^{-10}‡

* *Torr et al.* [1990]
† *Torr et al.* [1985]
‡ *Jones* [1974] (p. 115, 119)

types of emissions would thus be excited by lightning-induced heating: (*i*) emissions with duration determined by quenching efficiency (typical for the 'forbidden' transitions), having lower intensity since the radiation lasts longer than the radio impulse and most of the energy is taken off by quenching, (*ii*) emissions that last as long as the radio impulse (typical for the 'allowed' transitions), having substantially higher intensity since almost all the energy is radiated.

3. Results

We consider two cases of electron temperature distribution having a maximum temperature of respectively 6 eV (Case A) and 2 eV (Case B) at an altitude of ~93 km. According to *Inan et al.* [1991] and *Rodriguez et al.* [1992], Cases A and B respectively correspond to lightning electric field intensities of 10 V/m and ~5 V/m (normalized to 100 km of free space distance) [*Krider and Guo*, 1983]. The duration of the radio impulse from lightning (and hence the enhanced temperature) is taken to be 50 μs.

3.1. *Atomic Oxygen* (O)

We include the cascade from the ^1S state in the calculation of the population of the ^1D state but not the excitation of ^1S or ^1D states of O as a result of dissociation of the O_2 by electron impact due to lack of any firm data on these processes [*Zipf*, 1984; pp. 335-401].

The altitude distribution of the intensities of the red (6300 and 6364 Å) and green (5577 Å) lines is shown in Figure 3.

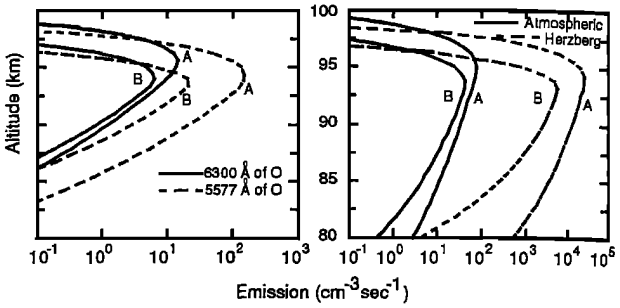

Fig. 3. (Left) Altitude distribution of the intensities of the 6300 (6364) Å (solid lines) and 5577 Å (dashed lines) emissions of atomic oxygen. The intensities of the lines for Case B are substantially lower than for Case A. Fig. 4. (Right) Same as Figure 3 for the O_2 atmospheric (solid lines) and Herzberg I (dashed lines) bands.

The exponential decay times of the intensity of the red and green lines are relatively short due to quenching of ^1D and ^1S states in collisions with neutral species (Table 1), respectively being ~1.5 ms (at ~96 km) and ~0.35 s (at ~95 km). For vertical (e.g., upward from ground) observations, the intensity of the red line is ~8 R for Case A and ~2.3 R for Case B whereas that for the green line is ~63 R for Case A and ~6.6 R for Case B.

3.2. *Molecular Oxygen* (O_2)

The atmospheric band of O_2 is very bright but is completely absorbed by O_2 in the lower atmosphere and can thus only be observed from altitudes above the stratosphere [*Torr et al.* 1985]. The Herzberg I band is the strongest UV feature of the night sky, but is heavily absorbed by ozone in the lower atmosphere. We only consider direct collisional excitation for both bands and downward observations from above the *D* region (i.e., spacecraft-based).

The intensities of the O_2 atmospheric and Herzberg I bands are shown in Figure 4. The exponential decay times of the atmospheric band and Herzberg I emissions are respectively ~6.5 s (at ~96 km) and ~90 ms (at ~95 km) and are determined by quenching of $b^1\Sigma_g^+$ and $A^3\Sigma_u^+$ states due to collisions with neutrals. For vertical (i.e., downward looking from spacecraft) observations the atmospheric band emits ~56 R

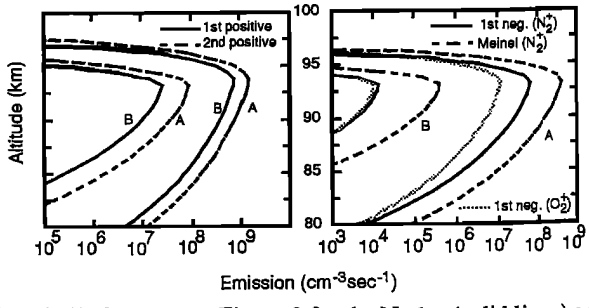

Fig. 5. (Left) Same as Figure 3 for the N_2 1st (solid lines) and 2nd positive (dashed lines) bands. Fig. 6. (Right) Same as Figure 3 for the 1st negative (solid lines) and Meinel (dashed lines) bands of N_2^+, and the 1st negative band of O_2^+ (dashed dotted lines).

for Case A and ~24 R for Case B whereas the Herzberg I band emits $\sim 1.6 \times 10^4$ R for Case A and $\sim 2.5 \times 10^3$ R for Case B.

3.3. *Molecular Nitrogen* (N_2)

For N_2 we consider the 1st and 2nd positive bands and neglect quenching of originating states by neutrals (see Table 1). Cascading from $C^3\pi_u$ to $B^3\pi_g$ state (resulting in the 2nd positive emissions) is included as the source for the 1st positive emissions.

The intensities of the N_2 1st positive and 2nd positive bands are shown in Figure 5. After termination of the radio impulse the exponential decay time of the intensity of the 1st and 2nd positive bands are respectively ~6 μs and ~50 ns as determined by radiation rates from the $C^3\pi_u$ and $B^3\pi_g$ states. For vertical (i.e., upward or downward looking) observations the 1st positive band emits $\sim 8.9 \times 10^8$ R for Case A and $\sim 3.6 \times 10^7$ R for Case B while the 2nd band emits $\sim 4.3 \times 10^8$ R for Case A and $\sim 9.5 \times 10^6$ R for Case B.

3.4. *Ions of Molecular Nitrogen and Oxygen* (N_2^+, O_2^+)

The 1st negative and Meinel bands of N_2^+, and the 1st negative band of O_2^+ are among the strongest auroral emissions [*Jones*, 1974; p. 125, 138]. However, the threshold energy these emissions is quite high (~16-19 eV; Figure 2).

The intensities of the N_2^+ 1st negative and Meinel bands, and the O_2^+ 1st negative bands are shown in Fig. 6. The exponential decay times for these bands are weakly influenced by quenching and are approximately equal to the inverse radiation rates given in Table 1 (i.e., ~70 ns for the N_2^+ 1st negative band, ~14 μs for the Meinel band, and ~1.2 μs for the O_2^+ 1st negative band). For vertical observations the 1st negative band of N_2^+ emits $\sim 2.6 \times 10^7$ R for the Case A and $\sim 4 \times 10^3$ R for Case B and the Meinel band emits $\sim 1.7 \times 10^8$ R for Case A and $\sim 1.2 \times 10^5$ R for Case B; the 1st negative band of O_2^+ has intensity $\sim 5.3 \times 10^6$ R for the Case A and $\sim 3.3 \times 10^3$ R for Case B.

Due to the high excitation threshold, the computed N_2^+ and O_2^+ emission intensities are particularly sensitive to the electron population in the high energy tail of the distribution. Thus, our assumption of a Maxwellian distribution is particularly critical for these emissions.

4. Discussion

That the longest emission time among the above is ~6 s indicates that relatively fast optical systems with 50μs to few seconds exposure time should be used, utilizing the intense radio impulse as a trigger. The size of the emitting region is important in estimating the intensity and duration of the optical pulse since the radiation time of the brightest emissions is small. For a ~500 km region [*Rodriguez et al.*, 1992] the pulse duration will spread from ~50 μs to 1.5 ms for limb and all-sky observations, due to the finite velocity of light.

4.1. *Emission Intensities Compared to Airglow*

The 6300 Å intensity for vertical observation is relatively low and is more than one order of magnitude less than the ambient intensity of the night airglow for vertical observations (~10^2 R [*Chamberlain*, 1978; p. 215]). However, the side view intensity for Case A (see Figure 3) is comparable to the ambient night airglow. The 5577 Å intensity for vertical observations is also comparable to the ambient night airglow (~10^2 R [*Chamberlain*, 1978; p. 215]), whereas the side view intensity (Figure 3) can be larger than the background level [*Thomas*, 1981]. The intensity of the O_2 atmospheric band is much below ambient levels ($\sim 3 \times 10^4$ R [*Chamberlain* 1978; p. 218]). The intensity of the Herzberg I band of O_2 (see Figure 4) is well above the background ($\leq$800 emission cm^{-3} s^{-1} [*Thomas*, 1981]) and could be measured from above the D region (downlooking from spacecraft).

Although the transitions of O and O_2 discussed above are quenched, the radiation and quenching time scales are much larger than the time of excitation by lightning radiation, so that the intensities of these lines are linearly proportional to the duration of the radio pulse.

The intensities of the N_2, N_2^+, and O_2^+ lines are several orders of magnitude larger than the background in corresponding spectral regions (~10^3 R [*Chamberlain*, 1978; pp. 214-218]).

In terms of detectability with typical auroral airglow photometers, we note that a good photometer would have a sensitivity of ~50 R-sec [*S. Mende*, private communication]. In this context, the N_2 emissions (Figure 5) of $10^7 - 10^9$ R, lasting for 50 μs correspond to 50-5,000 R-sec and should be detectable, while the 5577 Å line from O with ~60 R and ~350 ms duration is only ~27 R-sec which is marginal.

4.2. *Comparison with Boeck et al. [1992] Observations*

Recent observations from the Space Shuttle of lightning associated brightening in the airglow layer [*Boeck et al*, 1992] can be explained as electron impact induced emissions from the heated region above the thunderstorm. The images presented indicated an enhanced airglow region of ~500 km horizontal width ranging over a 10-20 km altitude range centered around ~95 km and it was pointed out that such events are relatively rare. Orientation and intensity of the lightning discharge determine the electron temperature and the vertical and horizontal extent of the heated region [*Rodriguez et al.*, 1992], and therefore the intensity and spectrum of subsequent emissions. Long lasting emissions from O and O_2 may not have been detected on the Space Shuttle for two reasons: (*i*) the wavelength for the brightest of them, Herzberg I band of O_2, lies outside the camera sensitivity region, (*ii*) the intensities of the 6300 Å and 5577 Å lines of O, and the atmospheric band of O_2, are below the sensitivity of the camera.

Each of the short lasting bands discussed above has transitions with wavelengths from 3600 Å to 7200 Å to which the TV cameras on the Space Shuttle were sensitive with peak sensitivity being at 4400 Å. Two lines of the 1st negative band of N_2^+ lie near the peak of the camera sensitivity. As is evident from Figure 6, for a 50 μs exciting pulse (resulting in 15 km of effective horizontal width of the emitting region of simultaneously registered photons) the side view intensity of this band averaged over a 10 km range in altitude is ~10^7 R for Case A and ~10^3 R for Case B. The duration of the emissions for the ~500 km width (as observed by [*Boeck et al*, 1992]) of the emitting region is ~1.5 ms. The effective intensity observable at the Space Shuttle would be ~10 times lower due to 1/60 s integration time of the camera resulting in ~10^6 R for Case A and ~10^2 for Case B. Case A

corresponds to electron heating for a ~10 V/m lightning intensity (at 100-km distance) for intracloud discharges or ~20 V/m for cloud-to-ground discharges [*Rodriguez et al.*, 1992], which occur ~10% of the time [*Krider and Guo*, 1983]. The emission intensities for less intense lightning would be below the background level, due to the relatively high thresholds (7.3 to 18.75 eV) of these transitions. Hence, the observed airglow transient [*Boeck et al*, 1992] probably consisted predominantly of unquenched N_2, N_2^+, and O_2^+ emissions, excited by a relatively intense (i.e., relatively rare) lightning discharge.

5. Summary

Lightning-induced heating of ionospheric electrons as discussed by *Inan et al.* [1991] is estimated to lead to the excitation of a number of emission lines from O, O_2, N_2, O_2^+, and N_2^+, with intensities ranging from $10 - 10^9$ R. For example, 5577 Å from O emits ~60 R and lasts for ~350 ms while the 1st and 2nd positive bands of N_2 emit ~10^9 R but last as long as the radio frequency pulse, namely ~50-100 μs.

The brightest emissions from the *D* region above a thunderstorm are expected to be the allowed transitions including the 1st and 2nd bands of N_2, the 1st negative and Meinel bands of N_2^+, and the 1st negative band of O_2^+. The radiation time of these bands is approximately equal to the duration of lighting stroke (i.e., 50 to 100 μs). For the emissions of O and O_2 considered, the radiation time is limited by quenching and does not exceed few seconds.

The N_2 and molecular ion lines would be best suited for observations from upward looking ground- or aircraft-based platforms whereas the O_2 lines would only be detectable from spacecraft. Most of the emissions appear to be easily detectable with fast optical systems with exposure times of 50 μs to several seconds, using the electromagnetic impulse from lightning to trigger the camera.

Acknowledgements. This work was supported by the Office of Naval Research under contracts N00014-82-K-0489 and N00014-92-J-1579. We thank our colleagues in the STAR Laboratory and S. Mende of Lockheed for useful discussions.

References

Boeck, W.L., O.H. Vaughan, Jr., R. Blakeslee, B. Vonnegut, and M. Brook, Lightning induced brightening in the airglow layer, *Geophys. Res. Lett.*, vol. 19, pp. 99-102, 1992.

Cartwright, D.C., W.R. Pendleton, Jr., and L.D. Weaver, Auroral emission of the N_2^+ Meinel bands, *J. Geophys. Res.*, vol. 80, pp. 651-654, 1975.

Cartwright, D.C., S. Trajmar, A. Chutjian, and W. Williams, Electron impact excitation of the electronic states of N_2. II. Integral cross sections at incident energies from 10 to 50 eV, *Phys. Rev. A*, vol. 16, pp. 1041-51, 1977.

Chamberlain, J.W., *Theory of planetary atmospheres*, Academic Press, New York, 1978.

Doering, J.P. and E.E. Gulcicek, Absolute differential and integral electron excitation cross sections for atomic oxygen 7. The $^3P \rightarrow {}^1D$ and $^3P \rightarrow {}^1S$ transitions from 4.0 to 30 eV, *J. Geophys. Res.*, vol. 94, pp. 1541-46, 1989.

Inan, U.S., T.F. Bell, and J.V. Rodriguez, Heating and ionization of the lower ionosphere by lightning, *Geophys. Res. Lett.*, vol. 18, pp. 705-708, 1991.

Jones, A.V., *Aurora*, D. Reidel publishing company, Dordrecht Holland, 1974.

Krider, E.P., and C. Guo, The peak electromagnetic power radiated by lightning return strokes, *J. Geophys. Res.*, vol. 88, p. 8471, 1983.

Reagan, J.B. et al, Modeling of the ambient and disturbed ionospheric media pertinent to ELF/VLF propagation, *Proc. of NATO-AGARD meeting on medium, long, and very long wave propagation*, Brussels, Belgium, September 1981.

Rees, M.H., *Physics and chemistry of the upper atmosphere*, Cabridge University Press, Cambridge, 1989.

Rodriguez, J.V., U.S. Inan, and T.F. Bell, *D* region disturbances caused by electromagnetic pulses from lightning, submittd to *Geophys. Res. Lett.*, 1992.

Thomas, R.J., Analyses of atomic oxygen, the green line, and Herzberg bands in the lower thermosphere, *J. Geophys. Res.*, vol. 86, pp. 206-210, 1981.

Torr, M.R, D.G. Torr, and R.R. Laher, The O_2 atmospheric 0-0 band and related emissions at night from Spacelab 1, *J. Geophys. Res.*, vol. 90, pp. 8525-38, 1985.

Torr, M.R., D.G. Torr, P.G. Richards, and S.P. Yung, Mid- and low-latitude model of thermospheric emissions 1. $O^+(^2P)7320Å$ and $N_2(2P)3371Å$, *J. Geophys. Res.*, vol. 95, pp. 21,147-68, 1990.

Watson, C.E., V.A. Dulock, Jr., R.S. Stolarski, and A.E.S. Green, Electron impact cross sections for atmospheric species. 3. Molecular oxygen, *J. Geophys. Res.*, vol. 72, pp. 3961-66, 1967.

Zipf, E.C., in *Electron-molecular interactions and their applications*, vol. 1, Academic Press, Inc., 1984.

Y. N. Taranenko, U. S. Inan and T. F. Bell, Space, Telecommunications And Radioscience Laboratory, Department of Electrical Engineering/SEL, Stanford University, Stanford, CA 94305.

(Received June 15, 1992;
Accepted August 26, 1992.)